Proceedings of DSCC2008
2008 ASME Dynamic Systems and Control Conference
October 20-22, 2008, Ann Arbor, Michigan, USA

DSCC2008-2248

MODEL-BASED FAULT DIAGNOSIS FOR NIMH

Chris Suozzo
Center for Automotive Research
and
Department of Electrical Engineering
The Ohio State University
suozzo.2@osu.edu

Simona Onori
Center for Automotive Research
The Ohio State University
onori.1@osu.edu

Giorgio Rizzoni
Center for Automotive Research
and
Department of Mechanical Engineering
The Ohio State University
rizzoni.1@osu.edu

ABSTRACT

The objective of this paper is to present a fault diagnosis methodology for hybrid electric vehicle battery systems. The faults that have been considered include: temperature sensor fault, current sensor fault, and voltage sensor. Many of these faults, if left undetected, will result in decreased battery performance and could eventually lead to pack failure.

INTRODUCTION

Nickel-metal hydride (NiMH) battery packs are one of the most costly components within a hybrid electric vehicle (HEV). The ability of these advanced batteries to maintain their power and energy characteristics for tens of thousands of miles is essential to ensure consumer acceptance of electrified powertrains. Achieving this level of continued performance and reliability is the responsibility of the battery management system (BMS), which prevents usage that would result in permanent damage to the battery pack. This oversight system is reliant on a number of sensors to assess the thermal and electrical state of the battery. A fault in one of these sensors can lead to an inaccurate evaluation of the battery's condition, causing the BMS to bring the pack into an unsafe operating regime. The purpose of the fault detection strategy developed herein is to identify whether a sensor fault is occurring, and then to isolate the source of the fault and alert the driver and/or BMS so that a corrective action can be taken before serious damage to the battery pack can occur. Demonstration of this approach to battery fault diagnosis will occur in simulation, and future work will include experimental validation.

BACKGROUND

Batteries allow for the storage of electrochemical energy, which can be converted into electrical energy when connected to a load or source. Chemical reactions inside a battery liberate electrons from the active material of one electrode so that they may be transported to the active material on another electrode by way of the outside circuit.

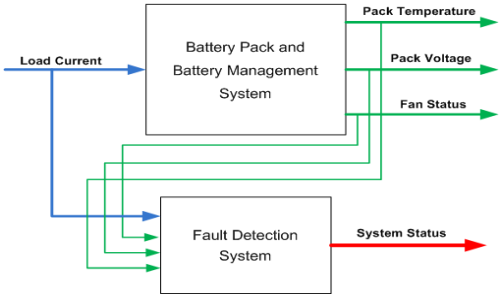

FIGURE 1. INPUT-OUTPUT DIAGRAM OF BATTERY PACK AND FAULT DETECTION SYSTEM.

A battery is said to be delivering power, or discharging, when electrical current is leaving the positive electrode (positive current flow). Conversely, when current is entering the positive electrode the battery is said to be charging (negative current flow), converting electrical energy to be stored in chemical form. The fundamental component in a battery pack is a cell. Each cell is comprised of a positive electrode, a negative electrode, electrolyte, a separator and frequently a case. The terminal voltage across the electrodes of a cell is unique to the cell's chemistry. Typical cell voltages are ~2V for lead-acid and ~1.2V for NiMH. A battery pack will typically connect a number of cells together in a series arrangement to increase the pack's voltage output. For the HEV battery pack under examination in this study, 250 cells have been placed in series, for a nominal pack voltage of approximately 300V.

The amount of energy a battery can store is easily calculated by multiplying its nominal voltage by the total number of amp-hours it can deliver. This last measurement of total charge (in terms of

amp-hours) is known as the battery's capacity. The capacity of the hybrid vehicle battery pack in this study is 10Ah. Knowledge of a battery's 'state of charge' (SOC) is very important for a battery management system. It is a measure of how many amp-hours the battery has been discharged divided by its nominal amp-hour capacity. It provides an indication of how many additional amp-hours the battery will be able to provide.

Battery Modeling

A battery's dynamic electrical behavior is highly dependent on the conditions under which it is operating. Temperature, state of charge and current directionality all contribute to the shape of a battery's voltage response to a given load current. Deviations from a battery's normal behavior can indicate the presence of a fault, and so it is important to be able to simulate the battery's ideal electrical and thermal characteristics under a variety of conditions.

The battery fault detection and isolation (FDI) methodology proposed in this study is a model-based approach. The nonlinear thermo-electric battery model developed in [1-3] and described in this section will be used to demonstrate the algorithm's performance in a simulation environment. The electrical model that is used for the battery in this study is a first order Randel model, represented in Figure 2. The dynamic electrical equations governing this circuit are Kirchhoff's current and voltage laws:

$$\frac{dV_C}{dt} = -\frac{V_C}{R_0 C_0} + \frac{I}{C_0}$$
$$V = E_0 - RI - V_C \qquad (1)$$

where V_C is the capacitor voltage, I is the current entering or leaving the positive terminal of the battery and V is the battery voltage measured at the terminals. For this particular model, the current I is treated as the input, and the output is the terminal voltage V.

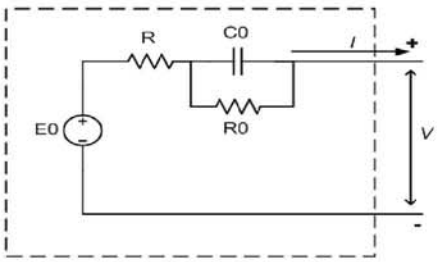

FIGURE 2. BATTERY ELECTRICAL MODEL.

Battery internal parameters include: resistance R, resistance R_0, capacitance C_0 and open-circuit voltage E_0. The values of these parameters are dependent on battery temperature, SOC and current directionality. Through a compilation of empirical data collected under a number of different operating conditions, the following relationships have been developed for a single battery cell [1-3]:

$$E_0 = 1.19 + 0.09 \cdot SOC + 0.001 \cdot T$$
$$C_0 = 1500$$
$$R = \begin{cases} 0.004 - 0.000044 \cdot T & if\ I > 0 \\ 0.004 - 0.000042 \cdot T & if\ I < 0 \end{cases} \qquad (2)$$
$$R_0 = \begin{cases} 0.0016 - 0.000025 \cdot SOC \cdot T & if\ I > 0 \\ 0.008 - 0.000022 \cdot T - 0.0036 \cdot SOC & if\ I < 0 \end{cases}$$

In addition to this electrical model, a simplistic state-of-charge estimator is needed. The easiest way of implementing this is by integrating the current entering or leaving the battery and then normalizing this quantity of charge with respect to the nominal capacity. This change in SOC can then be added or subtracted to the initial SOC to get an approximation of the present SOC.

$$SOC = SOC_0 + \Delta SOC$$
$$\Delta SOC = \frac{1}{Ah_{nom}} \int I(t)\, dt \qquad (3)$$

where Ah_{nom} is the nominal capacity of the battery. The initial SOC (SOC_0) can be found from a measurement of the rested open-circuit voltage (E_0) equation if the battery temperature T is known.

Finally, a simplistic thermal model of the battery is also identified. Current passing through the resistance in the battery electrical model generates heat, which is then transferred to the surrounding environment according to the equation:

$$\frac{dT}{dt} = \frac{R}{mc} I^2 + \frac{R_0}{mc} I_0^2 - \frac{hA}{mc}\left(T - T_{amb}\right) \qquad (4)$$

where I_0 is the current passing through R_0, T is the battery temperature, mc is the effective heat capacity per cell, hA is the effective heat transfer per cell and T_{amb} is the ambient temperature. High temperatures can be particularly problematic for batteries. On one hand, the internal resistance of a battery is lower at higher temperatures, allowing the battery to operate more efficiently.

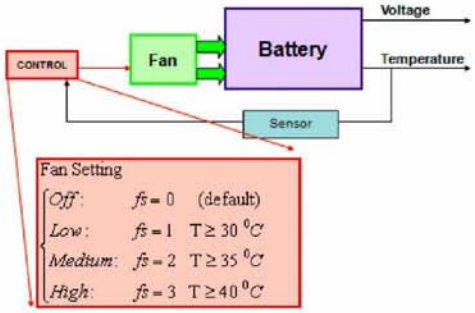

FIGURE 3. BATTERY TEMPERATURE CONTROL SYSTEM.

However, high temperatures cause a number of irreversible chemical reactions to take place in the battery which can result in capacity loss or increase in internal resistance.

To avoid this potentially life-shortening operating condition, hybrid vehicle battery packs are equipped with thermal management systems to maintain their operating temperature

within an acceptable range. For the purposes of this study, this component of the system will be represented by a thermostatically controlled fan with three speed settings to dissipate excess heat from the battery. This results in a slightly modified thermal equation, with the replacement of the heat transfer hA with an equation that is dependent on the fan speed:

$$hA = hA_0 \cdot \left(1 + \frac{f_s}{2}\right) \quad (5)$$

where hA_0 is the nominal heat transfer (0.07 J/K) due to natural convection and f_s is the fan setting, which takes an integer value from 0 to 3 depending on the battery temperature. The battery temperature control system is shown in Figure 3.

Damaging Operating Conditions

As was stated in the introduction, operation of a battery under certain conditions will dramatically reduce its useful lifetime. Frequent deep discharge and overcharging operation is known to cause capacity loss and increase in internal resistance. Similar performance losses occur during operation at high temperature. To avoid these undesirable operating conditions, the battery management system tracks of the battery's SOC by monitoring the battery voltage and current, and exercises its control authority to prevent it from falling below a predefined minimum value or rising above 100% SOC. In addition, the BMS activates a fan to dissipate excess heat from the battery pack when its temperature rises above 30°C. The ability of the BMS to maintain battery operation within the desired envelope is therefore highly dependent on accurate voltage, temperature and current measurements. It is the responsibility of the fault detection and isolation system to determine whether any of the sensors in the system are faulty.

Sensor Fault Simulation

To simulate the charge-sustaining nature of a hybrid vehicle battery pack loading cycle, a simple 5 step, 50A staircase is used to discharge the battery by a little over 8%, and then recharge the battery back up the original SOC (Figure 4). The first fault considered is that of the current sensor. During hybrid vehicle operation, it is common to track changes in the battery pack's state of charge by simply integrating the measured current with respect to time. If the current sensor's output is inaccurate, the state of charge estimation will suffer, and the BMS may allow the battery operate in a state that could cause permanent damage to the pack. Figure 5 illustrates the impact of a constant 3A 'drift' in the current measurement on the estimated SOC even over a short period.

Another fault that effects SOC estimation is that of the voltage sensor. When a battery is left open-circuit for a sufficiently long rest-period, it is possible to identify its SOC using a known relationship between rested open-circuit voltage and SOC. In an HEV, this condition could occur when the vehicle is left off overnight. Prior to vehicle operation, a rested open circuit voltage measurement can be used to determine the initial state of charge of the battery. Current integration is then used to track changes in SOC as the battery is charged and discharged. As seen in Figure 6, a fault in the voltage sensor will cause the BMU to incorrectly identify the initial SOC, and as a result damage to the pack due to overcharging or over discharging may occur.

The last fault injected into the simulation is of the temperature sensor. Figure 7 illustrates the problem well: temperature measurements that are lower than the actual battery temperature

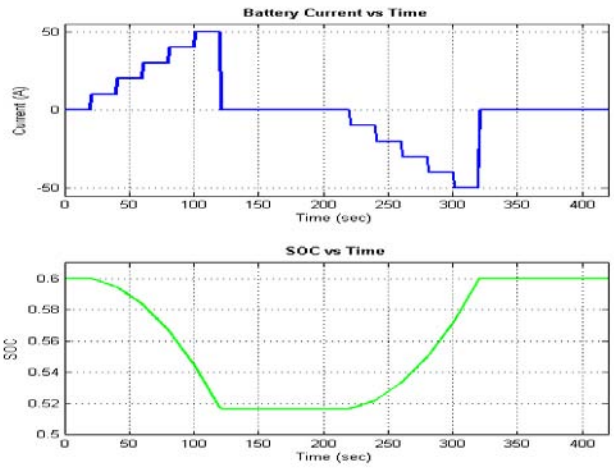

FIGURE 4. BATTERY INPUT CURRENT AND IDEAL CHANGE IN SOC.

FAULT DIAGNOSIS STRATEGY AND DESIGN

The strategy that has been formulated to detect and isolate sensor faults in a hybrid vehicle battery system is an observer-based approach. First, a linearized model of the battery was developed at several operating points. Generalized and input observers were then created to provide estimates of the measured signals that are used in residual generation. Primary residuals are calculated as the error between the sensor measurements and the observer estimates: $r_i = y_j - \hat{y}_j$.

Faults were then injected into the simulation and thresholds were set for each of the residuals. Finally, a unique set of residuals, or 'fault signatures', was identified for each fault to isolate the malfunctioning sensor.

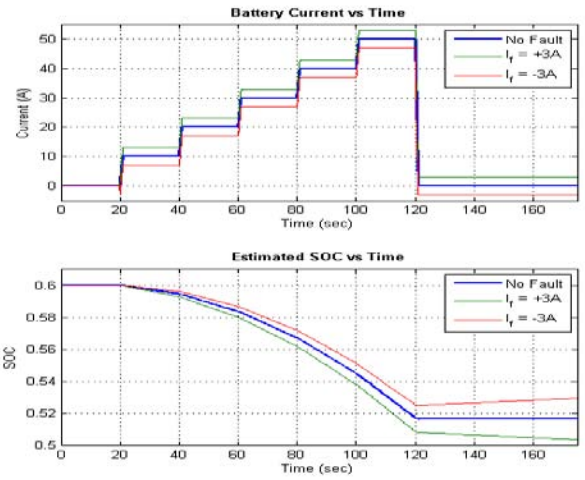

FIGURE 5. DISCHARGE CURRENT MEASUREMENT AND RESULTANT SOC ESTIMATION UNDER FAULT AND NO FAULT CONDITIONS. FAULT INJECTED AT 20 SECONDS.

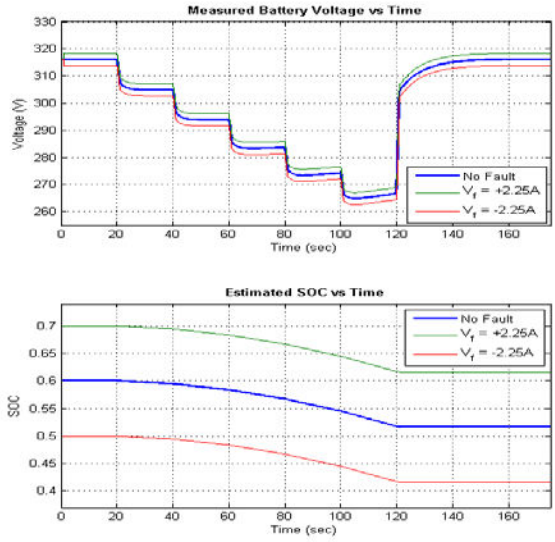

FIGURE 6. VOLTAGE MEASUREMENT DURING DISCHARGE STAIRCASE AND RESULTANT SOC ESTIMATION UNDER FAULT AND NO FAULT CONDITIONS.

Model Linearization

The states of this model are capacitor voltage V_C and battery temperature T, while battery current I and SOC are treated as the model inputs. The battery output voltage V and temperature T are the model outputs. The full extent of the nonlinearities in the electrical and thermal equations is revealed when electrical parameters E_0, R, and R_0 are substituted into the state and output equations. Linearization about the operating point I_0, SOC_0, T_0 and V_{C0} produces the follow state space system:

$$\dot{x} = \mathbf{A}x + \mathbf{B}u + e$$
$$y = \mathbf{C}x + \mathbf{D}u + f$$

$$\begin{bmatrix} \dot{V}_C \\ \dot{T} \end{bmatrix} = \begin{bmatrix} A_{11} & A_{12} \\ A_{21} & A_{22} \end{bmatrix} \begin{bmatrix} V_C \\ T \end{bmatrix} + \begin{bmatrix} B_{11} & B_{12} \\ B_{21} & B_{22} \end{bmatrix} \begin{bmatrix} I \\ SOC \end{bmatrix} + \begin{bmatrix} e_1 \\ e_2 \end{bmatrix}$$

$$\begin{bmatrix} V \\ T \end{bmatrix} = \begin{bmatrix} C_{11} & C_{12} \\ C_{21} & C_{22} \end{bmatrix} \begin{bmatrix} V_C \\ T \end{bmatrix} + \begin{bmatrix} D_{11} & D_{12} \\ D_{21} & D_{22} \end{bmatrix} \begin{bmatrix} I \\ SOC \end{bmatrix} + \begin{bmatrix} f_1 \\ f_2 \end{bmatrix}$$

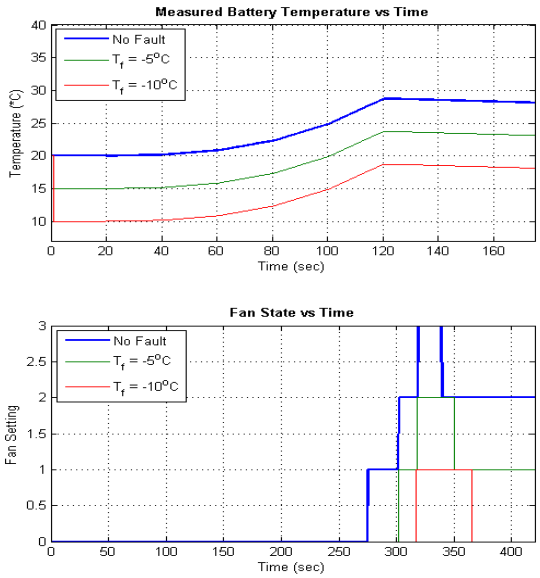

FIGURE 7. BATTERY TEMPERATURE AND FAN STATUS DURING TEMPERATURE SENSOR FAULTS.

The column vectors e and f are constant terms.

The range of possible current and capacitor voltage values encountered under a typical charge-sustaining HEV cycle widely between positive and negative values, depending on the demands of the driver. For the purposes of this study, the maximum current values experienced during discharge will be 155A for discharging, and -55A for charging. Similarly, the capacitor voltage will vary between positive and negative values during discharging and charging. Selecting one nominal value for either of these variables would severely impair the ability of the linearized model to accurately reproduce the battery's dynamic behavior throughout its range of operation. It was therefore decided that I_0, T_0 and V_{C0} would each switch between one of 10 different values depending on the operating condition.

Generalized Observer Scheme

The purpose of the generalized observers is to estimate the outputs of the system. These outputs are then compared to the measured outputs, and a fault determination can then be made from the error between these two signals. Each observer estimates

the i^{th} system output by using the input and all system outputs except for the i^{th}. The linearized battery model only has two outputs, *T* and *V,* and therefore only two observers were created. The output space was decomposed into:

$$y^{(1)} = \mathbf{C^{(1)}x} = \begin{bmatrix} C_{11} & C_{12} \end{bmatrix} \begin{bmatrix} V_C \\ T \end{bmatrix}$$

$$y^{(2)} = \mathbf{C^{(2)}x} = \begin{bmatrix} C_{21} & C_{22} \end{bmatrix} \begin{bmatrix} V_C \\ T \end{bmatrix}$$

The observer state estimation equations and their respective estimated outputs are then:

$$\textbf{Observer 1}: \ \dot{\hat{\mathbf{x}}} = \mathbf{A}\hat{\mathbf{x}} + \mathbf{B}\mathbf{u} + \mathbf{L}_1\left(y^{(1)} - \hat{y}^{(1)}\right)$$

$$\textbf{Observer 2}: \ \dot{\hat{\mathbf{x}}} = \mathbf{A}\hat{\mathbf{x}} + \mathbf{B}\mathbf{u} + \mathbf{L}_2\left(y^{(2)} - \hat{y}^{(2)}\right)$$

$$\text{where } \hat{y}^{(1)} = \hat{T}, \hat{y}^{(2)} = \hat{V}$$

Observer 1 uses the measured voltage *V* to estimate the temperature *T*, and observer 2 uses the measured *T* to estimate *V*. For the observer to be accurate under both charge and discharge conditions, two sets of gains were calculated for each observer. As the current directionality changes during simulation, so do the observer gains. Observer gains L were calculated using the *place()* command in MATLAB®.

The primary residuals derived from these observers, r_1 and r_2, are simply the difference between the output estimates and the actual measured values:

$$r_1 = T - \hat{T}; \ \ r_2 = V - \hat{V}$$

Input Observer

The generalized observer scheme allows us to find faults in the measurements of outputs *V* and *T*. The last fault we wish to investigate is that of the current sensor. To create an observer for *I*, the system output equation was rearranged:

$$V = C_{11} \cdot V_C + C_{12} \cdot T + D_{11} \cdot I + D_{12} \cdot SOC + f_1$$

$$\downarrow$$

$$I = -\frac{C_{11}}{D_{11}} \cdot V_C - \frac{C_{12}}{D_{11}} \cdot T + \frac{1}{D_{11}} \cdot V - \frac{D_{12}}{D_{11}} \cdot SOC - \frac{f_1}{D_{11}}$$

$$I = C_{11t} \cdot V_C + C_{12t} \cdot T + D_{11t} \cdot V + D_{12t} \cdot SOC + f_{1t}$$

In this form, the system output is now *I* and the measurement of *V* is used as the model input. Substitution of this equation into the state equations yields the new system:

$$\dot{V}_C = \left(A_{11} + B_{11} \cdot C_{11t}\right) \cdot V_C + \left(A_{12} + B_{11} \cdot C_{12t}\right) \cdot T + \left(B_{11} \cdot D_{11t}\right) \cdot V + \left(B_{12} + B_{11} \cdot D_{12t}\right) \cdot SOC + \left(e_1 + B_{11} \cdot f_{1t}\right)$$

$$\dot{T} = \left(A_{21} + B_{21} \cdot C_{11t}\right) \cdot V_C + \left(A_{22} + B_{21} \cdot C_{12t}\right) \cdot T + \left(B_{21} \cdot D_{11t}\right) \cdot V + \left(B_{22} + B_{21} \cdot D_{12t}\right) \cdot SOC + \left(e_2 + B_{21} \cdot f_{1t}\right)$$

An observer based on this new system was then created next using the same methodology used in the previous section.

$$\textbf{Observer 3}: \ \dot{\hat{\mathbf{x}}} = \mathbf{A}\hat{\mathbf{x}} + \mathbf{B}\mathbf{u} + \mathbf{L}\left(y - \hat{y}\right)$$

$$\text{where } \hat{y} = \hat{I}$$

The residual for the input observer is then defined to be:

$$r_3 = I - \hat{I}$$

Analysis of these three residuals under no fault and fault conditions will allow for the selection of appropriate thresholds that are sensitive to the faults.

RESULTS

In this section the performance of the observers under no fault and fault conditions will be examined. Thresholds were then selected for each residual. Residual values that exceed these thresholds indicate the presence of a fault.

Observer Performance

The performance of the observers designed in the previous section was tested in simulation, using the nonlinear model as the 'plant'. The simple discharge/charge staircase from Figure 5 was used as the input and no faults were injected.

Figures 8 shows that the observers are fairly accurate in their reproduction of the actual signals during both discharge and charge in the no fault condition.

RESIDUAL ANALYSIS

Residuals were generated for four different cases: no fault, voltage measurement fault, temperature measurement fault and current measurement fault. The smallest fault magnitudes that would result in damage to the pack were investigated in this section. The fault magnitudes were selected as follows: 1V for voltage sensor, -2°C for temperature sensor and 2A for current sensor. The voltage and current sensor faults would result in inaccurate SOC estimation that could result in overcharge or deep discharge conditions that would damage the pack. As shown in Section II, a temperature measurement lower than the actual battery temperature will result in later activation of the fan. This could cause the battery to overheat, and thus damage the pack. Figures 9 through 11 show each primary residual under fault and no fault conditions.

Thresholds were selected as follows:

Threshold for r_1 = $T_1 = -1.2$

Threshold for r_2 = $T_2 = \pm 0.6$

Threshold for r_3 = $T_3 = \pm 1.6$

A set of secondary residuals *d* is defined as follows. If a residual exceeds its threshold for more than 60 consecutive seconds, a fault is considered to have occurred. Under these conditions, the secondary residual will transition from its no fault state (0) to its fault state (1). Once this state transition occurs, the secondary residual *d* remains in the fault state indefinitely, or until the FDI system is manually reset. The secondary residual state transition from 0 to 1 indicates the presence of a fault. The next stage in the diagnosis process is to identify which sensor is faulty.

Table 1 provides the various fault signatures that can be linked to specific faults. Each fault has a unique signature defined by the status of the secondary residuals, and therefore fault isolation can be achieved.

Under the no fault condition, none of the secondary residuals were tripped. All primary residuals in the no fault condition were relatively small, and only during the large transients were the thresholds briefly exceeded. The voltage fault triggered secondary residual d_2. The temperature fault set both d_1 and d_2, and the current fault set residuals d_2 and d_3. For any set of secondary residual states not present in Table 1, the system will be able to detect a fault, but not isolate its source.

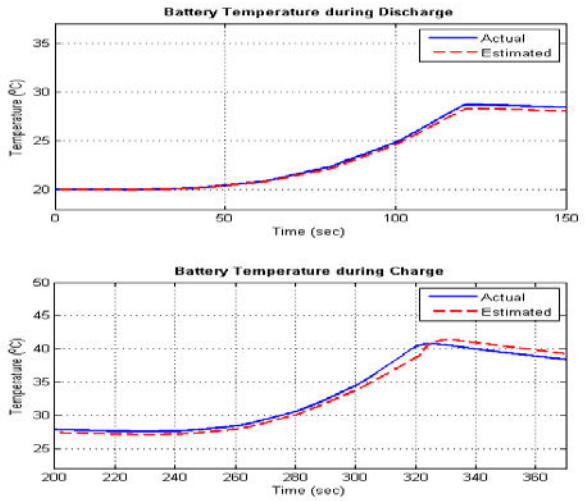

FIGURE 8. COMPARISON BETWEEN MEASURED AND ESTIMATED TEMPERATURES UNDER DISCHARGE AND CHARGE CONDITIONS.

CONCLUSION AND FUTURE WORK

The fault diagnostic strategy developed and demonstrated in this study successfully identified the presence of faults in voltage, temperature and current sensors. Furthermore, the secondary residuals provide a unique signature for each of these faults, allowing for identification of the faulty component. While this study only examined sensor faults and their consequences, there are a number of other faults in the battery system that could occur.

The FDI scheme described in this study could be expanded to uniquely identify more faults, including increases in the battery's internal resistance, connection resistance, and fan failure. Additional future work also includes the injection of various amounts of noise and model uncertainties into the simulation, and adjusting thresholds or fault signatures as necessary to eliminate the possibility of false alarms. Different current and temperature profiles consistent with actual HEV operation should also be tested. Nonlinear observers and adaptive thresholds are other promising techniques that could improve the system's diagnostic abilities, and therefore these fault detection methods should be explored to develop a more robust strategy. Lastly, experimental validation will occur when the FDI strategy has been satisfactorily evolved.

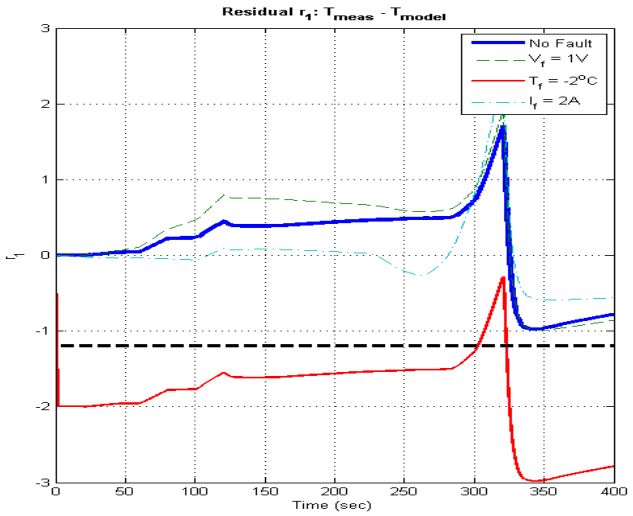

FIGURE 9. RESIDUAL R1 UNDER FAULT AND NO FAULT CONDITIONS.

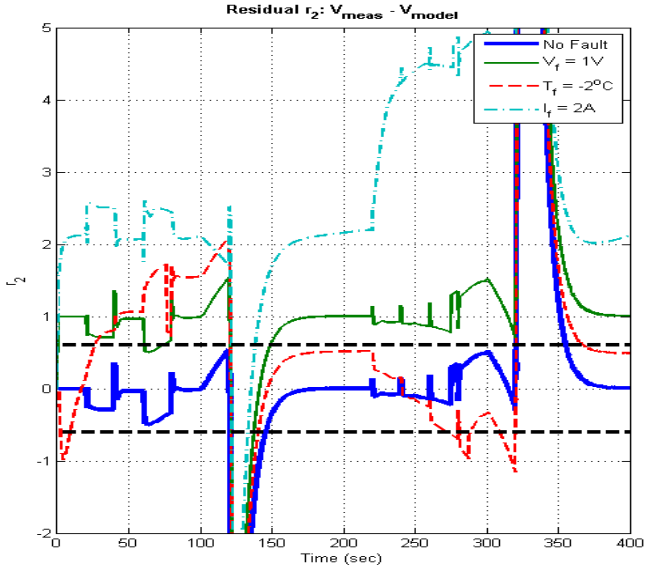

FIGURE 10. RESIDUAL R2 UNDER FAULT AND NO FAULT CONDITIONS.

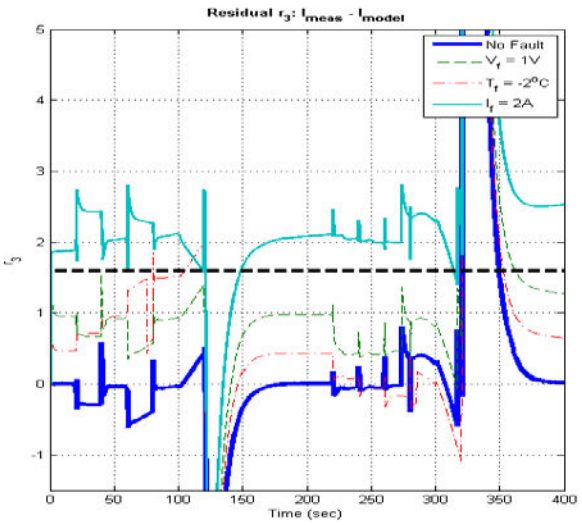

FIGURE 11. RESIDUAL R3 UNDER FAULT AND NO FAULT CONDITIONS.

TABLE 1
FAULT SIGNATURES

Fault Condition	d_1	d_2	d_3
No Fault	0	0	0
Voltage Sensor Fault	0	1	0
Temperature Sensor Fault	1	1	0
Current Sensor Fault	0	1	1

REFERENCES

[1] Chehab, Z., Serrao, L., Guezennec, Y., and Rizzoni, G., "Aging Characterization of Nickel-Metal Hydride Batteries Using Electrochemical Impedance Spectroscopy", *Proceedings of IMECE2006*, *2006 ASME*, November 5-10, 2006, Chicago, Illinois, USA.

[2] Storti, A., Bornatico, R., Zappavigna, A., Mandrioli, L., Guezennec, Y., and Rizzoni, G., "SoC Calibration and Validation for NiMH Batteries in HEV Operation", *Paper 2007-42484*, *ASME IMECE '07*, Seattle, WA, November 2007.

[3] Serrao, L., Chehab, Z., Guezennec, Y., and Rizzoni, G., "An Aging Model of NiMH Batteries for Hybrid Electric Vehicles", *Proc. IEEE Vehicle Power and Propulsion Conference*, Chicago, Illinois, September 2005.

[4] Paganelli, G., Guezennec, Y., Kim, H., and Brahma, A.. "Battery dynamic modeling and real-time state-of-charge estimation in hybrid electric vehicle application". *Symposium on advanced automotive technology-Dynamic system and control*. 2001, 11:11-16.